# Lithium restores inhibitory function and neuronal excitability through GSK-3β inhibition in a bipolar disorder-associated *Ank3* variant mouse model

René N. Caballero-Florán [a,1], Kendall P. Dean [b,1], Andrew D. Nelson [c], Lia Min [a], Paul M. Jenkins [a,d,*]

[a] Department of Pharmacology, University of Michigan Medical School, Ann Arbor, MI, 48109-5632, USA
[b] Cellular and Molecular Biology Program, University of Michigan Medical School, Ann Arbor, MI, 48109-5632, USA
[c] Weill Institute for Neurosciences, University of California, San Francisco, San Francisco, CA, 94143, USA
[d] Department of Psychiatry, University of Michigan Medical School, Ann Arbor, MI, 48109-5632, USA

## ARTICLE INFO

Handling Editor: Dr J Young

## ABSTRACT

Bipolar disorder (BD) is a prevalent psychiatric condition characterized by mood dysregulation, psychosocial impairment, and an increased risk of suicide. The gene *ANK3* has been identified as a risk locus for BD through multiple genome-wide association studies (GWAS). However, the mechanisms by which *ANK3* variants influence BD pathophysiology and treatment response remain unclear. *ANK3* encodes ankyrin-G, a protein that organizes the axon initial segment (AIS) and nodes of Ranvier by scaffolding ion channels and cell adhesion molecules to the cytoskeleton. Recent studies show that ankyrin-G interacts with the GABA$_A$ receptor-associated protein (GABARAP) to stabilize inhibitory synapses, potentially linking *ANK3* variants to inhibitory (GABAergic) signaling deficits associated with BD. We previously demonstrated that the BD-associated variant, *ANK3* p. W1989R, disrupts the ankyrin-G/GABARAP interaction, resulting in inhibitory deficits and cortical pyramidal neuron hyperexcitability in mice. In this study, we investigate how lithium, a common BD therapeutic, modulates neuronal excitability in this model. Our findings show that chronic lithium treatment selectively enhances presynaptic GABAergic neurotransmission, reduces neuronal hyperexcitability, and partially rescues AIS length, without altering the density of GABAergic synapses. We also show that the selective glycogen synthase kinase-3 beta (GSK-3β) inhibitor Tideglusib recapitulates the enhancement of presynaptic GABAergic signaling. These findings shed new light on how *ANK3* variants may contribute to inhibitory deficits in BD and demonstrate that lithium treatment is able to restore these deficits, likely through GSK-3β inhibition. Furthermore, these findings highlight GSK-3β inhibition as a promising therapeutic strategy for treating BD and other neurological disorders affected by GABAergic dysfunction.

## 1. Introduction

Bipolar disorder (BD) is a debilitating neuropsychiatric condition that affects approximately 2 % of the global population (Merikangas et al., 2011). It is characterized by recurrent episodes of mania or hypomania and depression, marked by significant alterations in mood and behavior (American Psychiatric Association, 2013; Organization, 1993). In addition to mood disturbances, BD is associated with cognitive and functional impairments that substantially reduce quality of life for affected individuals (Cullen et al., 2016; Oldis et al., 2016). BD is also linked to premature mortality, largely due to comorbidities such as cardiovascular disease (Roshanaei-Moghaddam and Katon, 2009) and an increased risk of suicide (Gonda et al., 2012; Schaffer et al., 2015).

Despite the severity and prevalence of the disorder, the mechanisms underlying BD development are not fully understood. Evidence suggests the etiology of the disorder involves a combination of genetic, environmental, and neurochemical factors, leading to abnormalities in neuroanatomical structure and neuronal signaling (Carvalho et al.,

2020). The heritability of BD is estimated to be as high as 85 %, underscoring the significant role of genetics in susceptibility (Smoller and Finn, 2003). Several genome-wide association studies (GWAS) have identified the gene *ANK3* as a significant risk locus for the disorder (Ferreira et al., 2008; Lee et al., 2011; Muhleisen et al., 2014; Mullins et al., 2021; Psychiatric GWAS Consortium Bipolar Disorder Working Group, 2011; Stahl et al., 2019). However, the precise mechanisms through which BD-associated *ANK3* variants contribute to the disorder and influence patient responses to BD therapeutics remain unclear.

*ANK3* encodes the protein ankyrin-G, which plays a critical role in the formation of excitable membrane domains in neurons (Bennett and Lorenzo, 2013; Nelson and Jenkins, 2017; Stevens and Rasband, 2021). Ankyrin-G mediates the assembly and function of the axon initial segment (AIS) and nodes of Ranvier by scaffolding voltage-gated Na+ and K+ channels to facilitate action potential (AP) generation and propagation in these regions (Jenkins and Bender, 2025; Nelson and Jenkins, 2017; Smith and Penzes, 2018; Stevens and Rasband, 2022). Additionally, ankyrin-G stabilizes inhibitory (GABAergic) synapses at the AIS and soma of neurons by interacting with the $GABA_A$ receptor-associated protein (GABARAP), preventing endocytosis of $GABA_A$ receptors (Nelson et al., 2020; Tseng et al., 2015).

Inhibitory (GABAergic) signaling is important for maintaining homeostasis of neuronal circuits and proper brain function, and deficits in GABAergic signaling have been implicated across multiple psychiatric disorders, including BD (Fatemi et al., 2013, 2017; Ozerdema et al., 2013; Schubert et al., 2015; Torrey et al., 2005). It is unknown whether common BD therapeutics, including lithium treatment, can reverse these deficits in inhibitory signaling. Lithium has been used in mood disorder treatment since its discovery in the mid-20th century (Shorter, 2009), and despite its limitations and side effects (Gitlin, 2016), it remains the gold standard for BD treatment (Fountoulakis et al., 2017; Yatham et al., 2018). Lithium monotherapy is effective for treating and preventing mania (Fountoulakis et al., 2022; Nestsiarovich et al., 2022) and is associated with anti-suicidal effects (Cipriani et al., 2013). Although lithium has been used as a therapeutic agent for over 60 years, the exact mechanisms underlying its effects remain under investigation.

Lithium has been shown to regulate a variety of cellular pathways involved in synaptic plasticity, brain circuitry, and neurotransmission (Bortolozzi et al., 2024). Many of these effects are thought to be mediated through lithium's role as a glycogen synthase kinase-3 beta (GSK-3β) inhibitor (Bortolozzi et al., 2024). GSK-3β is a critical regulator of cellular homeostasis, and its dysregulation has been implicated in several disorders, including BD (Beurel et al., 2015; Jope and Johnson, 2004). Lithium inhibits GSK-3β both directly, by occupying a magnesium binding site on the enzyme, and indirectly, by increasing GSK-3β phosphorylation (Bortolozzi et al., 2024). While lithium treatment has been shown to regulate various cellular pathways through this mechanism, its effects on GABAergic signaling in the context of BD remain poorly understood.

Previously, we characterized a mouse model harboring the *Ank3* p.W1989R variant, originally identified in a family with BD, which abolishes the interaction between ankyrin-G and GABARAP (Nelson et al., 2020). *Ank3* p.W1989R mice display a significant reduction in the number of GABAergic synapses on the soma and AIS of cortical pyramidal neurons, as well as decreased forebrain gamma oscillations, indicative of reduced inhibitory function (Nelson et al., 2020; Tseng et al., 2015). Cortical pyramidal neurons from these mice also exhibit deficits in GABAergic neurotransmission, marked by a reduction in the frequency and amplitude of inhibitory post synaptic currents (IPSCs) (Nelson et al., 2020). This loss of inhibitory tone results in an increase in AP firing frequency and shortened AIS length, indicative of pyramidal neuron hyperexcitability (Nelson et al., 2020). Collectively, these results suggest that this *ANK3* variant may contribute to BD etiology through disrupted GABAergic signaling. Additionally, this raises the possibility that BD therapeutics, including lithium treatment, may function to restore these deficits and mitigate neuronal hyperexcitability.

This study investigates whether lithium treatment can restore GABAergic function and neuronal excitability in our previously described mouse model harboring the *Ank3* p.W1989R BD-associated variant. We demonstrate that chronic lithium treatment restores the frequency, but not the amplitude, of inhibitory postsynaptic currents (IPSCs) in *Ank3* p.W1989R mice. Lithium treatment also does not affect the density of GABAergic synapses, suggesting that it selectively enhances presynaptic GABAergic neurotransmission without affecting post-synaptic receptors in this mouse model. This enhancement of presynaptic GABA release is sufficient to normalize pyramidal neuron firing frequency and partially rescue AIS length abnormalities, indicating an overall reduction in neuronal hyperexcitability. Furthermore, the specific GSK-3β inhibitor Tideglusib mimicked the effects of chronic lithium treatment, enhancing presynaptic GABAergic neurotransmission without impacting postsynaptic properties, supporting a role of GSK-3β inhibition in modulating GABAergic activity. In contrast to chronic lithium treatment, the effects of Tideglusib were found to be AP-independent, suggesting differences between lithium therapy and specific GSK-3β inhibition.

This study demonstrates that chronic lithium treatment restores presynaptic GABAergic signaling and rescues neuronal hyperexcitability in *Ank3* p.W1989R mice likely through GSK-3β inhibition, highlighting GSK-3β inhibition as a promising therapeutic target for restoring neuronal function in BD and other mood disorders characterized by GABAergic dysfunction.

## 2. Materials and methods

### 2.1. Animals

*Ank3* p.W1989R mice were described previously (Nelson et al., 2020). *Ank3* p.W1989R heterozygous male and female mice were crossed to generate respective genotypes and littermates were used for all experiments. Animals were group housed (2–5 per ventilated cage) with 24-h (12/12 dark/light cycle) access to food and water. Mice were maintained on a 12:12 light:dark schedule with lights turning on at 5am (6am during Daylight Savings Time). Litters from the heterozygous breeders were weaned at postnatal day 21 (P21) and raised to P42-48. For mice that underwent lithium therapy, lithium chow was provided at P21, while control mice were fed with regular chow (vehicle), as described below. All experimental procedures were performed with the guidelines for animal care of the institutional animal care and use committee (IACUC), and university laboratory animal management (ULAM) at the University of Michigan.

### 2.2. Pharmacological treatments and measurement of plasma lithium levels

Littermates of both sexes were fed with regular chow or 0.2 % (g/kg chow) lithium carbonate diet (Harlan Teklad TD.170313/12) for 14 days followed by 7 days of 0.36 % (g/kg chow) to achieve lithium therapeutic levels as described previously (Zhu et al., 2017). During lithium treatment, each cage of mice was supplemented with an extra bottle of 0.9 % NaCl to reduce the risk of dehydration and the bedding was changed daily. For Tideglusib treatment, mice were administrated Tideglusib (Sigma-Aldrich, St. Louis, MO, USA) or vehicle (corn oil; Sigma-Aldrich, St. Louis, MO, USA) via subcutaneous injection every other day for 20 days (20 mg/kg body weight) (Fuchs et al., 2018). Electrophysiology recordings were carried out the next day following cessation of treatment and to maintain consistency in our results, tissue was collected at a standard time (9–10am) for slice electrophysiology experiments. Blood was collected immediately after euthanasia and saved in tissue plasminogen activator (TPA)/heparin (100 μL). Samples were sent to the University of Michigan clinical core to measure serum lithium concentration.

## 2.3. *In vitro electrophysiology recordings*

Mice were anesthetized with isoflurane and decapitated (all procedures are by approved UM IACUC protocol PRO00010191). The brain was quickly removed from the skull and placed in 4 °C slicing solution (in mM): 62.5 NaCl, 2.5 KCl, 1.25 $KH_2PO_4$, 26 $NaHCO_3$, 5 $MgCl_2$, 0.5 $CaCl_2$, 20 glucose and 100 sucrose (pH = 7.4 with $O_2/CO_2$ 95/5 %, ~315 mOsm). The location of the somatosensory cortex in coronal brain slices was identified according to the mouse brain atlas by Paxinos and Franklin(Paxinos and Franklin, 2019), and coronal slices (~300 μm thick) containing somatosensory cortical layers II/III were cut on a microtome (VF-300, CompresstomeTM; Precisionary instruments, Natick MA). All recordings were taken from the same brain region.

Brain slices were transferred to a chamber maintained at room temperature in artificial cerebrospinal fluid (ACSF) (in mM): 125 NaCl, 2.5 KCl, 1.25 $KH_2PO_4$, 26 $NaHCO_3$, 1 $MgCl_2$, 2 $CaCl_2$, and 20 glucose, pH 7.4 and ~300 mOsm, for at least 1 h before recording. Individual slices were transferred to a recording chamber perfused with ACSF (1–2 mL/min). Recording micropipettes were pulled for a final resistance of 5–7 MΩ (P-97; Sutter Instruments, Novato, CA) from borosilicate glass capillaries (1.5 mm O.D.; Harvard Apparatus, Holliston, MA) and filled with solution (in mM): 135 K-Gluconate, 4 NaCl, 0.4 GTP, 2 Mg-ATP,0.5 $CaCl_2$, 5 EGTA and 10 HEPES, pH 7.25, ~290 mOsm. The neurons were identified optically using a Nikon Eclipse FN-1 microscope with a 40× water-immersion objective and a DAGE-MTI IR-1000 video camera. Neurons were characterized using IR-DIC to evaluate their orientation, morphology, and spiking properties. Signals were recorded with Axoclamp 700B amplifier (Axon Instruments, Union City, CA), low pass filtered at 10 kHz. Whole-cell patch-clamp recordings were performed on cells with a high cell resistance (>8 GΩ before break-in). Current clamp recordings were obtained and analyzed from neurons in layers II/III of somatosensory cortex as previously reported (Nelson et al., 2020). For voltage-clamp experiments, putative LII/III pyramidal cells were selected for recording based on somatic pyramidal morphology and the presence of an apical dendrite emerging from the soma towards the pia. For current-clamp experiments, identical anatomical criteria were applied before establishing whole-cell recordings. Pyramidal cell identity was then confirmed by recording AP responses to somatic current injection. All cells exhibited regular spiking features, with AP accommodation and a lack of fast AP afterhyperpolarization that distinguishes pyramidal cells from parvalbumin and somatostatin interneurons, suggesting that targeting of cells by anatomical features in slice can allow one to record preferentially from excitatory cells. All data were acquired at 20 kHz with a 10 kHz Bessell filter (Multiclamp 700B, Molecular Devices).

The neurons were recorded by applying negative and positive current pulses of 10 pA for 1000 ms to calculate the rheobase (minimum current to fire the first AP) and the maximum firing frequency response, and single positive pulses of 1 ms to measure single AP properties as previously described (Nelson et al., 2020). For GABAergic currents, the K-gluconate in the internal solution was replaced with CsCl [140 mM], and the recordings were acquired at 2 kHz holding at −70 mV. Spontaneous inhibitory postsynaptic currents (sIPSCs) and miniature inhibitory postsynaptic currents (mIPSCs) were pharmacologically isolated using the AMPA/kainite receptor antagonist 6-cyano-7-nitroquinoxaline-2,3-dione (CNQX) [10 μM], and the NMDA antagonist DL-2-Amino-5-phosphonopentanoic acid (DL-AP-5) [100 μM]. The use of CNQX and DL-AP-5 pharmacologically isolates sIPSCs by specifically blocking excitatory signals, thereby mitigating potential interference with the measurement of inhibitory currents. To assess mIPSCs, the perfusion was supplemented with 1 μM Tetrodotoxin (TTX) to inhibit synaptic responses reliant on action potentials. Continuous monitoring of access resistance was conducted during the experiment, and trials were terminated if changes exceeding 20 % were observed. The analysis entailed assessing the frequency and amplitude of these events, as described earlier. The events were automatically detected using Minianalysis (Synaptosoft Inc.) and were visually examined to eliminate any potential erroneous noise (Nelson et al., 2020).

## 2.4. *Immunocytochemistry of brain sections*

After 21 days of lithium treatment, P42 mice were administered a ketamine/xylazine mixture (80 mg/kg body weight ketamine and 10 mg/kg xylazine) via intraperitoneal injection. The mice were euthanized by cardiac perfusion of PBS followed by 4 % paraformaldehyde and the brain was immediately removed and fixed overnight in 4 % paraformaldehyde. The next day, the brains were processed using a standard single-day paraffin preparation protocol (PBS wash followed by dehydration through 70, 95, and 100 % ethanol with final incubations in xylene and hot paraffin under vacuum) using a Leica ASP 300 paraffin tissue processor. Paraffin sections were cut at 7 μm thickness using a Leica RM2155 microtome and placed on glass slides. Sections were deparaffinized and rehydrated using a standard protocol of washes: 3 × 4-min xylene washes, 2 × 2-min 100 % ethanol washes, and 1 × 2-min 95 %, 80 %, and 70 % ethanol washes followed by at least 5 min in ddH₂O. Antigen retrieval was then conducted by boiling the deparaffinized brain sections for 20 min in 10 μM sodium citrate in a microwave oven. Sections were cooled, washed for 15 min in ddH₂O, rinsed in PBS for 5 min, and blocked using blocking buffer (5 % BSA, 0.2 % Tween 20 in PBS) for 1 h at room temperature. Slides were incubated overnight at 4 °C with primary antibodies diluted in a blocking buffer. On the following day, slides were washed 3 times for 15 min with PBS containing 0.2 % Tween 20, incubated with secondary antibodies diluted in blocking buffer for 1 h at room temperature, washed 3 times for 15 min, and mounted with Prolong Gold. Samples were imaged on a Zeiss LSM 880 with a 63X NA1.4 Oil/DIC Plan-Apochromat objective at 488, 561, and 647 nm lasers. AIS length and GABAergic synapse number were measured using maximum intensity projections of z-stacks. We only quantified AISs that were entirely contained within the bounds of the Z-stack. The number of vGAT-positive puncta was quantified above a set fluorescence intensity consistent across all samples. N refers to the number of mice used in the experiment, whereas n refers to the total number of neurons measured.

## 2.5. *Statistical analysis*

Statistical analysis was conducted using GraphPad Prism (Version 8.0) software. To assess the significance of differences between groups, Unpaired t-tests and ANOVAs were employed, with verification that the results adhered to the assumptions of normality and homogeneity of variances using the Shapiro-Wilk and Bartlett tests, respectively. We presented our statistical results by elucidating the specifics of the applied statistical tests, including the statistical value, degrees of freedom, and the exact p-value, tailored to the specific test used. In cases where the Gaussian distribution criterion was not met, the Kruskal-Wallis test with Dunn's post hoc analysis was applied. When inequality of variances was identified, Welch's ANOVA was used, followed by the post hoc Dunnett's test. In all instances, the criterion for statistical significance was set at Alpha (α) = 0.05. For tests with observations of statistical significance post-hoc power analyses were conducted using G Power (3.1). These analyses considered the alpha level, sample size based on the group average, and effect size to compute the achieved equivalent statistical power (1- beta (β) error probability) of 0.8 or higher.

## 3. Results

### 3.1. *Chronic lithium treatment does not affect the density of GABAergic synapses on the soma or axon initial segment (AIS) of Ank3 p.W1989R cortical pyramidal neurons*

GABAergic interneurons are essential for synchronizing neural

networks and mediating higher-order cognitive functions in the brain (Buzsaki and Wang, 2012; Tamas et al., 2000). Disruptions in GABAergic signaling have been implicated in a variety of neuropsychiatric disorders, including BD (Fatemi et al., 2013, 2017; Ozerdema et al., 2013; Schubert et al., 2015; Torrey et al., 2005). Previously, we demonstrated that *Ank3* p.W1989R mice exhibit a significant reduction in the number of GABAergic synaptic clusters on the soma and AIS of cortical pyramidal neurons (Nelson et al., 2020). To investigate whether chronic lithium treatment can reverse these deficits, we performed immunohistochemistry on coronal brain sections from wild type (WT), *Ank3* p.W1989R (WR), and *Ank3* p.W1989R mice treated with lithium for 21 days (WR + Li). 21 days of lithium treatment was previously shown to rescue a subset of behavioral deficits in *Ank3* null mice (Zhu et al., 2017). *Ank3* p.W1989R littermates given lithium reached plasma lithium levels of: 1.07 ± 0.039 mmol/L after treatment, concentrations similar to those recommended for patients undergoing lithium therapy (Nolen et al., 2019). Inhibitory synapses were identified by staining for the vesicular GABA transporter (vGAT), while ankyrin-G was used label the AIS (Fig. 1A). As expected, *Ank3* p.W1989R mice displayed a significant reduction in the density of GABAergic synaptic clusters on both the soma and AIS of pyramidal neurons (Fig. 1B and C) (Nelson et al., 2020). However, chronic lithium treatment did not restore the density of inhibitory synapses in these regions (Fig. 1). These findings prompted us to explore whether lithium treatment can affect other aspects of

inhibitory neurotransmission in this mouse model, independent of changes in GABAergic synapse density.

### 3.2. Chronic, but not acute, lithium treatment increases the frequency of spontaneous inhibitory postsynaptic currents (sIPSCs) in Ank3 p.W1989R mice

To determine if lithium treatment rescues GABAergic function in *Ank3* p.W1989R mice, we performed whole-cell patch-clamp recordings on cortical sections from WT, *Ank3* p.W1989R, and *Ank3* p.W1989R mice treated with lithium for 19–21 days. Consistent with previous findings, both the frequency and amplitude of spontaneous inhibitory postsynaptic currents (sIPSCs) were reduced in cortical pyramidal neurons in *Ank3* p.W1989R mice compared to WT mice (Fig. 2A–C) (Nelson et al., 2020). After 21 days of lithium treatment, the amplitude of sIPSCs remained unchanged in *Ank3* p.W1989R mice (Fig. 2A–C). However, the frequency of sIPSCs in *Ank3* p.W1989R mice was rescued to levels observed in WT counterparts (Fig. 2A–C), reflecting an increase in presynaptic GABA release from cortical interneurons following chronic lithium treatment. WT mice treated with chronic lithium showed no significant changes in the frequency or amplitude of sIPSCs, indicating that lithium does not increase presynaptic GABA release in WT mice as it does in *Ank3* p.W1989R mice (Fig. S1). Furthermore, this effect is dependent on chronic lithium administration, as acute lithium exposure
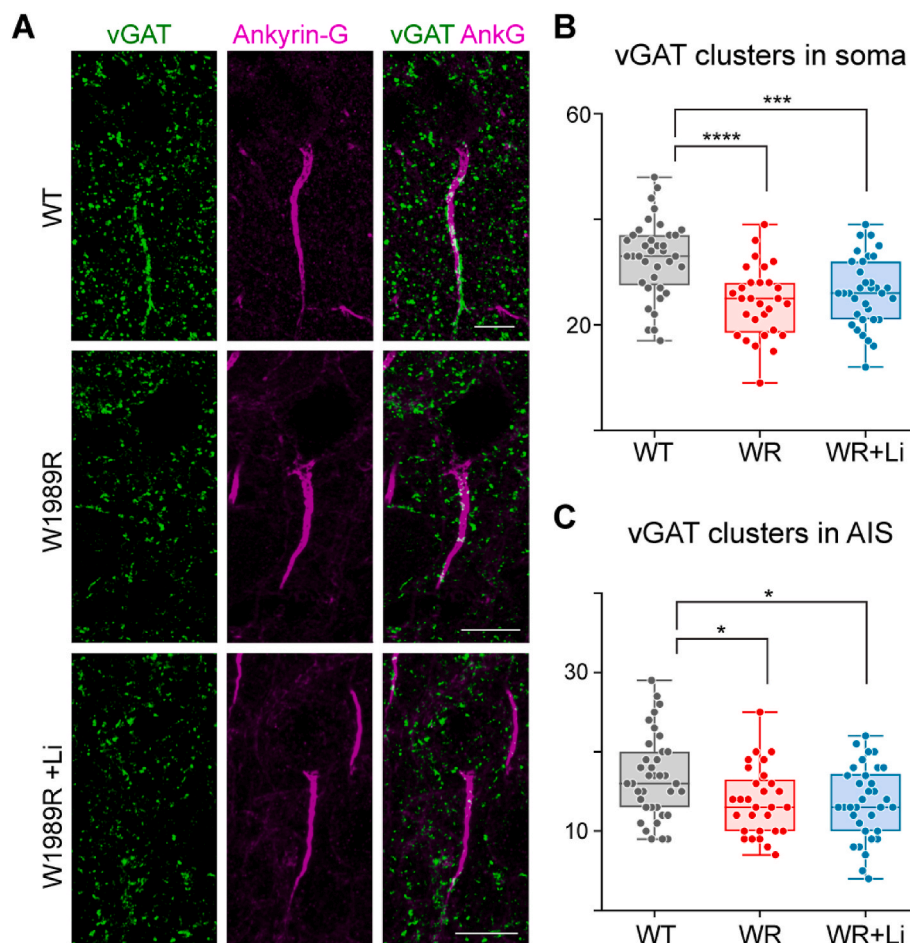


**Fig. 1. Lithium treatment does not affect the density of GABAergic synapses on the soma or axon initial segment (AIS) of cortical pyramidal neurons in *Ank3* p.W1989R mice.** (A) Representative images of GABAergic synapses on pyramidal neurons in layer II/III somatosensory cortex of wild type (WT), *Ank3* p.W1989R (W1989R), and *Ank3* p.W1989R mice following 21 days of lithium treatment (W1989R + Li). Coronal brain sections were immunostained with a presynaptic GABAergic marker vGAT (green) and total ankyrin-G (magenta). Scale bars: 10 μm. (B) Quantification of the total number of vGAT-positive clusters per soma above a set intensity threshold from WT (gray), *Ank3* p.W1989R (WR) (red), and lithium treated *Ank3* p.W1989R (WR + Li) (blue). (C) Quantification of AIS vGAT-positive clusters from WT (gray), WR (red), and WR + Li (blue). One-way ANOVA: ****P < 0.0001, ***P = 0.0004 and P = ns (WT: n = 37; WR: n = 29; WR + Li: n = 34).
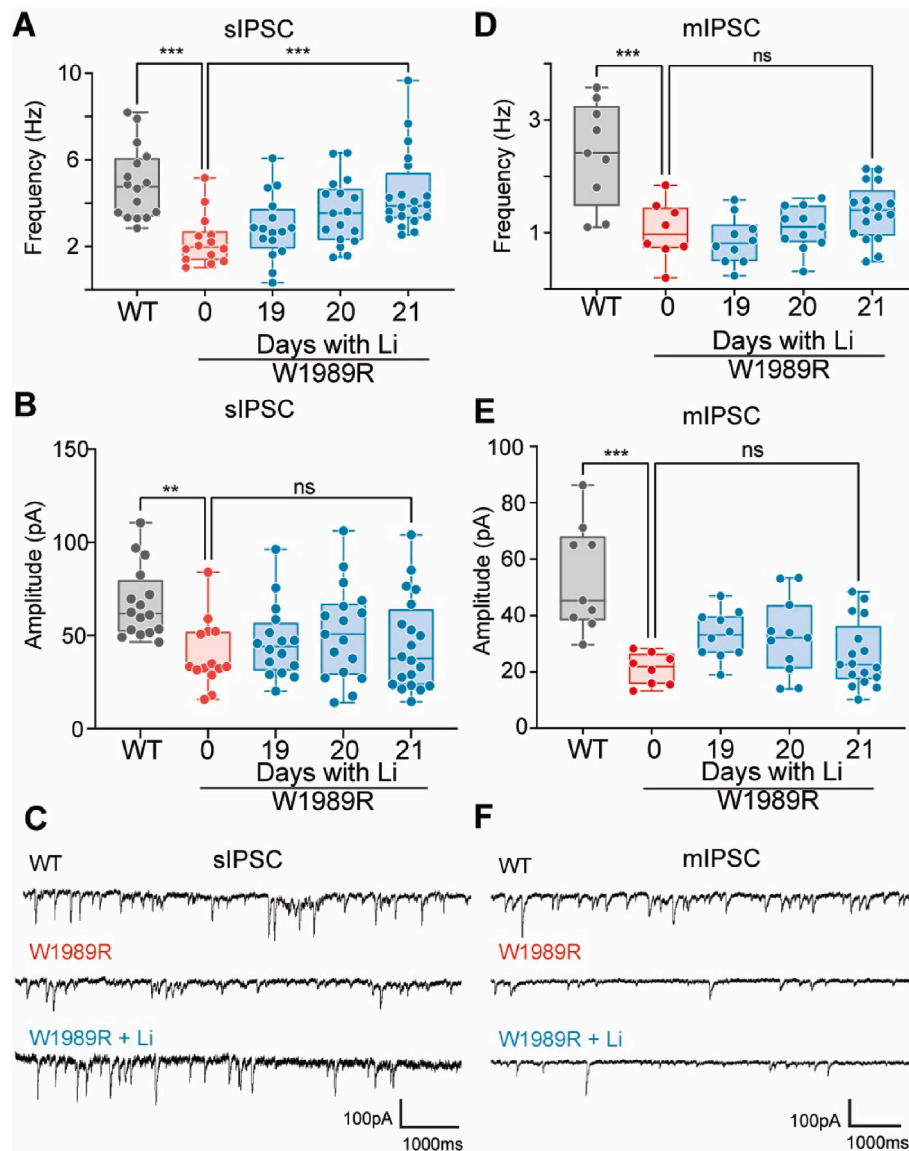
**Fig. 2. Chronic lithium treatment increases IPSC frequency, while not affecting current amplitude, in *Ank3* p.W1989R mice.** (A) Quantification of sIPSC and frequency (Hz) and (B) amplitude (pA) from cortical neurons from brain slices of wild type (WT) (gray), *Ank3* p.W1989R (W1989R) (red), and *Ank3* p.W1989R (W1989R) after chronic lithium treatment 19–21 days (blue). Kruskal-Wallis, Dunn's multiple comparisons test ***P < 0.01 and P = ns (WT: n = 16; W1989R: n = 15; W1989R/Day 19 + Li: n = 16; W1989R/Day 20 + Li: n = 17 and W1989R/Day 21 + Li n = 20). (C) Representative traces of sIPSC plots (A) and (B). (D) Quantification of mIPSC frequency (Hz) and amplitude (E) of WT (gray), W1989R (red), and W1989R after chronic lithium treatment 19–21 days (blue). Ordinary one-way ANOVA, Tukey's multiple comparisons tests: ***P < 0.001, and P = ns. (WT: n = 9; W1989R: n = 8; W1989R/Day 19 + Li: n = 10; W1989R/Day 20 + Li: n = 11 and W1989R/Day 21 + Li n = 17). (F) Representative traces of mIPSC in (D) and (E).

did not rescue sIPSC frequency in *Ank3* p.W1989R mice (Fig. S2). These results indicate that chronic, but not acute, lithium treatment selectively enhances presynaptic GABAergic transmission in this mouse model.

### 3.3. Chronic lithium treatment does not alter miniature inhibitory postsynaptic currents (mIPSCs) in Ank3 p.W1989R mice

To examine whether alterations in GABAergic transmission following chronic lithium treatment are AP-independent, we measured mIPSCs in the presence of TTX. Excitatory pyramidal neurons in *Ank3* p.W1989R cortical sections exhibited significantly reduced mIPSC frequency and amplitude compared to those from WT, consistent with previous findings (Fig. 2D–F) (Nelson et al., 2020). Interestingly, chronic lithium treatment did not restore the frequency or amplitude of mIPSCs in *Ank3* p.W1989R mice (Fig. 2D–F), indicating that lithium's effects on GABAergic transmission are dependent on AP firing in this model.

WT mice treated with chronic lithium also showed no significant changes in the frequency or amplitude of mIPSCs (Fig. S1). Additionally, no sex-related differences were observed following lithium treatment (Fig. S3). Collectively, these results suggest that chronic, but not acute, lithium therapy selectively enhances presynaptic GABAergic transmission from interneurons in *Ank3* p.W1989R mice in an AP-dependent manner, without impacting the amplitude of postsynaptic currents recorded from pyramidal neurons.

### 3.4. Tideglusib increases the frequency of sIPSCs and mIPSCs in Ank3 p. W1989R mice

Inhibition of GSK-3β is a key mechanism thought to mediate lithium's therapeutic effects (Bortolozzi et al., 2024), and Tideglusib is an approved GSK-3β inhibitor (Dominguez et al., 2012; Fuchs et al., 2018; Morales-Garcia et al., 2012; Sereno et al., 2009). To determine if the

effects of lithium treatment on presynaptic GABAergic function are recapitulated by specific GSK-3β inhibition, we treated *Ank3* p.W1989R mice with Tideglusib for 20 days and measured sIPSCs and mIPSCs in layer II/III cortical pyramidal neurons. Tideglusib treatment resulted in an increase in both sIPSC and mIPSC frequency in *Ank3* p.W1989R mice (Fig. 3A–C, D, F), with no impact on the amplitude of either sIPSCs or mIPSCs (Fig. 3B, C, E, F). These findings demonstrate that, like chronic lithium treatment, specific GSK-3β inhibition enhances presynaptic GABAergic neurotransmission in *Ank3* p.W1989R mice without altering postsynaptic receptor properties. Interestingly, unlike chronic lithium treatment, the effects of Tideglusib on inhibitory signaling appear to be AP-independent, as demonstrated by the increase in mIPSC frequency following Tideglusib treatment (Fig. 3). These results suggest that GSK-3β inhibition is likely an important mechanism underlying lithium's modulation of presynaptic GABAergic neurotransmission. However, key differences exist between lithium and Tideglusib treatment, particularly regarding the AP-dependence of this process.

### 3.5. Chronic lithium treatment restores action potential firing rate and frequency in Ank3 p.W1989R mice

To assess the impact of chronic lithium treatment on pyramidal neuron excitability, we compared evoked AP firing frequency in WT, *Ank3* p.W1989R, and *Ank3* p.W1989R mice treated with lithium for 21 days. Consistent with previous findings, *Ank3* p.W1989R mice exhibited significantly increased AP firing frequencies in response to escalating current injections, compared to WT mice (Fig. 4A and B) (Nelson et al., 2020). Additionally, the maximum firing frequency of *Ank3* p.W1989R neurons was significantly higher than that of WT neurons (Fig. 4C). Following chronic lithium treatment, both the firing rates across different current injections and the maximum firing frequency of APs were restored to levels observed in WT mice (Fig. 4A, B, C). Cell membrane and AP properties were not affected after lithium treatment (Fig. S4). While the threshold of the first AP generated from the AP train was significantly more depolarized in lithium-treated *Ank3* p.W1989R mice compared with WT mice, this difference was not seen in single

evoked APs (Fig. S4). These data indicate that chronic lithium treatment restores pyramidal neuron excitability in *Ank3* p.W1989R mice to levels seen in WT mice without affecting single AP properties.

### 3.6. Chronic lithium treatment partially restores AIS length deficits in Ank3 p.W1989R mice

The axon initial segment (AIS) is dynamically regulated in response to neuronal activity, and alterations in AIS morphology can reflect changes in neuronal signaling and network activity (Huang and Rasband, 2018). Excitatory pyramidal neurons from *Ank3* p.W1989R mice exhibit a shortened AIS, which is thought to serve as a compensatory mechanism for neuronal hyperexcitability (Nelson et al., 2020). To assess whether lithium treatment impacts AIS morphology, we quantified the length of the AIS in layer II/III cortical pyramidal neurons from WT, *Ank3* p.W1989R, and *Ank3* p.W1989R mice treated with lithium for 21 days. Ankyrin-G immunostaining was used to identify the AIS in each sample. Interestingly, lithium treatment resulted in a significant increase in AIS length in *Ank3* p.W1989R mice, although it remained shorter than that of WT mice (Fig. 5A–B). This partial restoration of AIS length may reflect lithium's ability to mitigate neuronal hyperexcitability in *Ank3* p.W1989R mice, thereby reducing the need for compensatory mechanisms such as AIS shortening.

## 4. Discussion

Bipolar disorder (BD) is a prevalent psychiatric disorder, characterized by behavioral dysregulation and elevated risk of suicide. The gene *ANK3*, encoding ankyrin-G, has been identified as a significant risk locus for BD through multiple genome-wide association studies (GWAS). However, the precise mechanisms by which variants in *ANK3* contribute to BD pathophysiology, as well as their influence on treatment response, remain incompletely understood.

Previously, we demonstrated that the *ANK3* p.W1989R variant, identified in a BD patient cohort, leads to impaired inhibitory signaling and neuronal hyperexcitability in mice. Specifically, *Ank3* p.W1989R
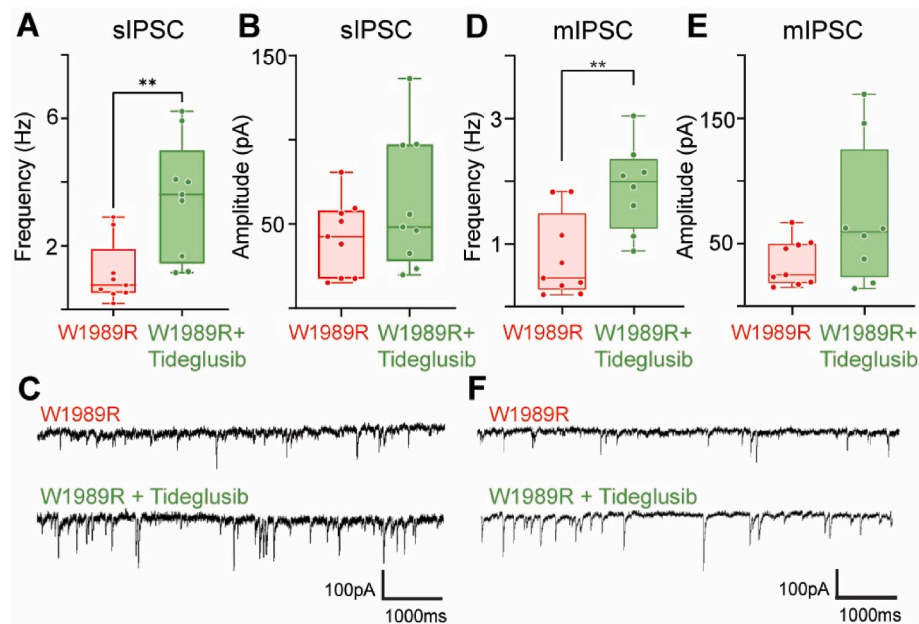
**Fig. 3. Chronic Tideglusib treatment increases sIPSC and mIPSC frequency while not affecting current amplitude in *Ank3* p.W1989R mice.** (A) Quantification of sIPSC frequency (Hz) and (B) amplitude (pA) from cortical neurons from brain slices of *Ank3* p.W1989R (W1989R) (red), and *Ank3* p.W1989R (W1989R) with Tideglusib treatment (green). Unpaired *t*-test **P < 0.005 (W1989R + vehicle: n = 9; and W1989R + Tideglusib n = 9). (C) Representative traces of sIPSC in (A) and (B). (D) Quantification of mIPSC frequency (Hz) and (E) amplitude (pA) from cortical neurons from brain slices of *Ank3* pW1989R (W1989R) (red), and *Ank3* pW1989R (W1989R) chronic Tideglusib treatment (green). Unpaired *t*-test **P < 0.005 (W1989R + vehicle: n = 9; and W1989R + Tideglusib n = 9) (F) Representative traces of mIPSC plots (D) and (E).
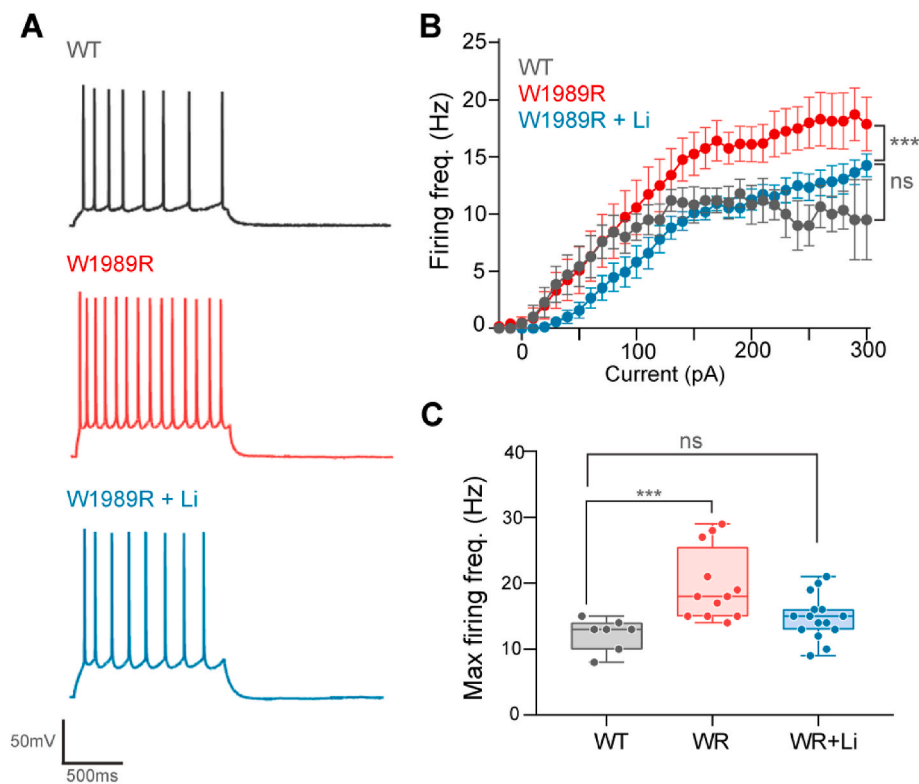
**Fig. 4. Pyramidal neuron firing frequency is restored in *Ank3* p.W1989R mice following chronic lithium treatment.** (A) Representative traces of APs generated by current injection in wild type (WT) (gray), *Ank3* p.W1989R (WR) (red), and *Ank3* p.W1989R after lithium treatment (WR + Li) (blue) neurons. (B) Average firing rate (Hz) vs. current injection (pA) from evoked APs in cortical neurons from wild type (WT) (gray), *Ank3* p.W1989R (W1989R) (red), and *Ank3* p. W1989R after lithium treatment (W1989R + Li) (blue). Two-way ANOVA, Tukey's multiple comparisons tests: WT vs. W1989R ***P < 0.001, WT vs. W1989R + Lithium P = ns, and W1989R vs. W1989R + Lithium ***P < 0.001. (C) Maximum firing frequency (Hz) graph of pyramidal neurons from WT (gray), *Ank3* p.W1989R (WR) (red), and *Ank3* p.W1989R after lithium treatment (WR + Li) (blue). Kruskal-Wallis, Dunn's multiple comparisons tests: WT vs. W1989R ***P < 0.001, WT vs. W1989R + Lithium P = ns, W1989R + Lithium vs W1989R P < 0.05 (WT: n = 7; W1989R: n = 12; W1989R + Li: n = 15).
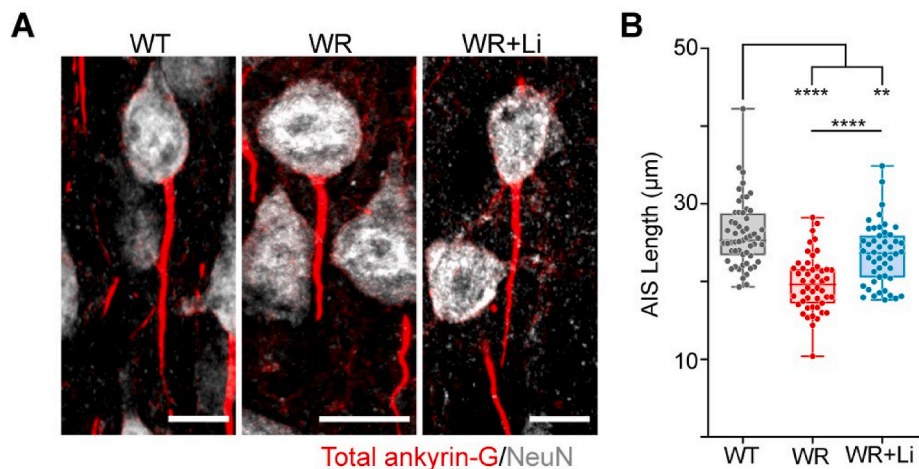


**Fig. 5. Lithium treatment increases the AIS length in *Ank3* p.W1989R mice.** (A) Representative images of pyramidal neuron AIS length from layer II/III somatosensory cortex of wild type (WT), *Ank3* p.W1989R (WR), and *Ank3* p.W1989R following lithium treatment (WR + Li). Immunostaining for total ankyrin-G (red) and NeuN (white). Scale bars: 10 μm. (B) Quantification of AIS length between WT (gray), WR (red), and WR + Li (blue). One-way ANOVA: ****P < 0.0001, ****P < 0.0001 and **P = 0. 0033 (WT: n = 55; WR: n = 48; WR + Li: n = 48).

mice display reduced GABAergic synaptic density, reduced IPSC frequency and amplitude, and increased AP firing rate compared to WT neurons. These deficits were identified in cortical and hippocampal, but not cerebellar or thalamic neurons, in this mouse model (Nelson et al., 2020). In the present study, we investigate how chronic lithium treatment modulates neuronal excitability and inhibitory signaling in this model, focusing on neuronal signaling deficits identified previously in the cortex. Previously we reported that the *Ank3* p.W1989R mice exhibit GABAergic signaling deficits in pyramidal cells from layer II/III somatosensory cortex, which fall within the sensorimotor network (Nelson et al., 2020). The sensorimotor network includes motor cortex, cingulate cortex, and sensory areas of the neocortex (somatosensory, auditory,

and visual) (Bi et al., 2022). Although the exact brain regions that underly the etiology of bipolar disorder remain incompletely understood, evidence suggests that deficits in emotion, cognition, and psychomotor activity observed in bipolar disorder can be linked to irregularities in several cortical and subcortical regions, including the sensorimotor network (Bi et al., 2022).

In this study, we find that chronic treatment with the bipolar disorder therapeutic, lithium, selectively enhances presynaptic inhibitory signaling and alleviates several hallmarks of neuronal hyperexcitability in this cortical region. Here we show that chronic lithium treatment in *Ank3* p.W1989R mice selectively augments presynaptic interneuron-mediated GABAergic neurotransmission, reduces pyramidal neuron hyperexcitability, and partially restores abnormalities in AIS length, without affecting GABAergic synapse density. We also demonstrate that treatment with the selective glycogen synthase kinase-3 beta (GSK-3β) inhibitor, Tideglusib, produces similar results, enhancing presynaptic GABAergic neurotransmission. These findings suggest that both chronic lithium treatment and selective GSK-3β inhibition may exert therapeutic effects in BD patients by enhancing interneuron-mediated GABAergic signaling, thus mitigating neuronal hyperexcitability.

Lithium is one of the front-line treatments for patients with bipolar disorder (Fountoulakis et al., 2017; Yatham et al., 2018). However, lithium treatment is not effective for all patients with bipolar disorder (Gitlin, 2016), and the exact mechanisms of lithium's mood stabilizing effects remain under investigation. GSK-3β inhibition is one of the known targets of lithium (Bortolozzi et al., 2024). It is unknown what exact neurochemical changes occur as a result of lithium treatment and GSK-3β inhibition, and how these changes may contribute to neuronal excitability and mood stabilization. Therefore, we sought to determine what the exact impact of lithium treatment and specific GSK-3β inhibition through Tideglusib would be in this mouse model. Testing the impact of lithium treatment and GSK-3β inhibition in this mouse model is of particular interest as patients with bipolar disorder often experience deficits in inhibitory signaling, and the *Ank3* p.W1989R variant results in a specific loss of inhibitory synapses, and functional deficits in inhibitory signaling. Therefore, to develop new more effective therapeutics, it is important to understand what similarities and differences may exist between specific GSK-3β inhibition and lithium treatment, which impacts various cellular processes in addition to GSK-3β.

Our results demonstrate that chronic lithium treatment in *Ank3* p.W1989R mice selectively increases the frequency, but not amplitude, of sIPSCs. This suggests that lithium treatment induces an increase in GABA release from presynaptic terminals without altering postsynaptic receptor properties. Lithium treatment is thought to activate neurotrophic cascades through GSK-3β inhibition, BDNF/TrkB signaling, and mTOR activation which produce bioenergetic stimuli necessary for synaptic plasticity (Bortolozzi et al., 2024). This increase in bioenergetic stimuli may contribute to the increase in pre-synaptic GABA release from interneurons observed in the *Ank3* p.W1989R mice treated with lithium. Interestingly, the GSK-3β inhibitor Tideglusib produced similar effects, enhancing the frequency of sIPSCs. This is likely due to the shared mechanism of GSK-3β inhibition between lithium and Tideglusib. GSK-3β is a key regulator of synaptic plasticity and neuronal signaling, and its inhibition has been shown to exert therapeutic effects in the treatment of BD and other mood disorders (Bortolozzi et al., 2024). These findings suggest that the effects of lithium on GABAergic signaling in *Ank3* p.W1989R mice are likely mediated, at least in part, by GSK-3β inhibition. Interestingly, our results suggest that GSK-3β inhibition alone is sufficient to increase pre-synaptic GABA release, as Tideglusib treatment rescued deficits in IPSC frequency similarly to lithium treatment. This reinforces the growing body of evidence that supports GSK-3β as a critical target in BD treatment and underscore its potential as a therapeutic pathway for modulating GABAergic function in BD.

While both chronic lithium and Tideglusib treatments restored sIPSC frequency, only Tideglusib was able to rescue deficits in mIPSC frequency observed in *Ank3* p.W1989R mice. This is particularly noteworthy, as, unlike sIPSCs, mIPSCs are measured in the presence of the sodium channel inhibitor TTX, which blocks AP firing. While both lithium and Tideglusib inhibit GSK-3β, the differences in their effects on AP-dependent versus AP-independent processes may be attributed to the broader spectrum of effects lithium has on neuronal excitability, whereas Tideglusib's more selective inhibition of GSK-3β likely produces more localized changes in neurotransmission that are independent of AP firing. Neither chronic lithium nor Tideglusib treatment was able to restore the amplitude of mIPSCs, reinforcing the notion that neither is capable of modulating postsynaptic receptor properties in this mouse model.

The density and function of postsynaptic inhibitory receptors influence the amplitude of inhibitory post-synaptic currents (IPSCs). The *Ank3* p.W1989R mutation disrupts the interaction between ankyrin-G and GABARAP, which results in enhanced endocytosis of the GABA_A receptor and a reduction in the number of inhibitory synapses (Nelson et al., 2020; Tseng et al., 2015). Gephyrin, one of the main scaffolding proteins involved in the stabilization of inhibitory synapses, is phosphorylated by GSK-3β, and inhibition of GSK-3β through lithium treatment has been shown to increase gephyrin clustering at inhibitory synapses (Tyagarajan et al., 2011). While the exact relationship between gephyrin and ankyrin-G at inhibitory synapses remains unclear, an increase in gephyrin clustering through GSK-3β inhibition could potentially stabilize GABA synapses to overcome deficits associated with *Ank3* p.W1989R. However, we find that lithium treatment is unable to restore deficits in GABAergic synapse density in this mouse model. This observation raises further questions about the relationship between these scaffolding proteins and their role in stabilizing GABAergic synapses, as these findings suggest that increased gephyrin clustering alone cannot restore the number of inhibitory synapses, at least in this *Ank3* p. W1989R variant model.

Several studies have explored the impact of lithium treatment on *Ank3*-deficient mice (Garza et al., 2018; Gottschalk et al., 2017; Piguel et al., 2023). While this study provides compelling evidence for the role of chronic lithium treatment in modulating GABAergic neurotransmission and neuronal excitability in *Ank3* p.W1989R mice, it is important to note that mice do not fully recapitulate all aspects of BD pathology. While, we have yet to characterize behavioral deficits in the *Ank3* p. W1989R mouse line, previous work from our collaborators and our group has shown that *Ank3* knockout mice exhibit mania-like behaviors that reverse with lithium treatment in the same timeframe used in these studies (Zhu et al., 2017). Additionally, sleep disruption is a common phenotype in many neuropsychiatric disorders, including BD, and abnormal sleep patterns have been observed in mice harboring a BD-associated *Ank3-1b* deletion variant (Villacres et al., 2023). Characterizing sleep abnormalities and their potential mediation by lithium treatment in this mouse model could offer further insights into how lithium therapies influence BD patient behavior. Furthermore, while GSK-3β inhibition appears to play a key role in modulating GABAergic transmission, other lithium-sensitive signaling pathways may also contribute to its therapeutic effects and should be explored in future studies. Future studies employing human-derived model systems could help bridge the gap between animal models and BD patients.

Our results demonstrate that chronic lithium treatment partially restores inhibitory deficits, normalizing the excitability of cortical pyramidal neurons, without altering the number of inhibitory synapses in a BD-patient *ANK3* variant mouse model. Furthermore, we find that this restoration of excitatory and inhibitory balance is, at least in part, due to the inhibition of GSK-3β, a key mediator of lithium's therapeutic action. These findings provide new insights into how lithium treatment may enhance inhibitory signaling and promote therapeutic effects in BD patients, contributing to the growing body of research implicating GSK-3β inhibition as a primary mechanism underlying lithium's mood-stabilizing effects. By further investigating how GSK-3β inhibition enhances inhibitory signaling and integrating mouse studies with BD patient-derived neurons, we may be able to develop more targeted and

effective therapeutic strategies for BD that not only address the symptoms but also specifically restore the underlying neuronal deficits.

## 5. Conclusions

In summary, alterations in the BD-associated gene *ANK3* and its encoded protein, ankyrin-G, are implicated in the presentation of BD symptoms. Our findings demonstrate that chronic treatment with lithium or Tideglusib restores deficits in GABAergic signaling through GSK-3β inhibition, enhancing neuronal inhibitory transmission helping to reinstate pyramidal excitability. This study offers insights into the underlying pathophysiology of genetic variants in *ANK3* that confer susceptibility to BD. It also sheds light on how dysregulated neuronal function in BD can be restored by treatments targeting GSK-3β, providing valuable knowledge that may facilitate the development of more effective BD therapies, novel medications, and the selection of optimal treatment approaches.

## CRediT authorship contribution statement

**René N. Caballero-Florán:** Writing – original draft, Methodology, Investigation, Formal analysis, Data curation, Conceptualization. **Kendall P. Dean:** Writing – review & editing, Formal analysis, Data curation. **Andrew D. Nelson:** Investigation, Formal analysis, Conceptualization. **Lia Min:** Writing – review & editing, Project administration. **Paul M. Jenkins:** Writing – review & editing, Writing – original draft, Validation, Supervision, Project administration, Funding acquisition, Formal analysis, Conceptualization.

## Declaration of competing interest

The authors declare the following financial interests/personal relationships which may be considered as potential competing interests: Paul Jenkins has received research funding from Neuropharmaka and is a consultant for Flux Therapeutics.

## Acknowledgments

## Appendix A. Supplementary data

Supplementary data to this article can be found online at https://doi. org/10.1016/j.neuropharm.2025.110649.

## Data availability

Data will be made available on request.

## References

American Psychiatric Association, 2013. Diagnostic and Statistical Manual of Mental Disorders. Washington, DC.

Bennett, V., Lorenzo, D.N., 2013. Spectrin- and ankyrin-based membrane domains and the evolution of vertebrates. Curr. Top. Membr. 72, 1–37.

Beurel, E., Grieco, S.F., Jope, R.S., 2015. Glycogen synthase kinase-3 (GSK3): regulation, actions, and diseases. Pharmacol. Ther. 148, 114–131.

Bi, B., Che, D., Bai, Y., 2022. Neural network of bipolar disorder: Toward integration of neuroimaging and neurocircuit-based treatment strategies. Transl Psychiatr. 12, 143.

Bortolozzi, A., Fico, G., Berk, M., Solmi, M., Fornaro, M., Quevedo, J., Zarate Jr., C.A., Kessing, L.V., Vieta, E., Carvalho, A.F., 2024. New advances in the pharmacology and toxicology of lithium: a neurobiologically oriented overview. Pharmacol. Rev. 76, 323–357.

Buzsaki, G., Wang, X.J., 2012. Mechanisms of gamma oscillations. Annu. Rev. Neurosci. 35, 203–225.

Carvalho, A.F., Firth, J., Vieta, E., 2020. Bipolar disorder. N. Engl. J. Med. 383, 58–66.

Cipriani, A., Hawton, K., Stockton, S., Geddes, J.R., 2013. Lithium in the prevention of suicide in mood disorders: updated systematic review and meta-analysis. BMJ 346, f3646.

Cullen, B., Ward, J., Graham, N.A., Deary, I.J., Pell, J.P., Smith, D.J., Evans, J.J., 2016. Prevalence and correlates of cognitive impairment in euthymic adults with bipolar disorder: a systematic review. J. Affect. Disord. 205, 165–181.

Dominguez, J.M., Fuertes, A., Orozco, L., del Monte-Millan, M., Delgado, E., Medina, M., 2012. Evidence for irreversible inhibition of glycogen synthase kinase-3beta by tideglusib. J. Biol. Chem. 287, 893–904.

Fatemi, S.H., Folsom, T.D., Rooney, R.J., Thuras, P.D., 2013. Expression of GABAA alpha2-, beta1- and epsilon-receptors are altered significantly in the lateral cerebellum of subjects with schizophrenia, major depression and bipolar disorder. Transl. Psychiatry 3, e303.

Fatemi, S.H., Folsom, T.D., Thuras, P.D., 2017. GABA(A) and GABA(B) receptor dysregulation in superior frontal cortex of subjects with schizophrenia and bipolar disorder. Synapse 71, e21973.

Ferreira, M.A., O'Donovan, M.C., Meng, Y.A., Jones, I.R., Ruderfer, D.M., Jones, L., Fan, J., Kirov, G., Perlis, R.H., Green, E.K., Smoller, J.W., Grozeva, D., Stone, J., Nikolov, I., Chambert, K., Hamshere, M.L., Nimgaonkar, V.L., Moskvina, V., Thase, M.E., Caesar, S., Sachs, G.S., Franklin, J., Gordon-Smith, K., Ardlie, K.G., Gabriel, S.B., Fraser, C., Blumenstiel, B., Defelice, M., Breen, G., Gill, M., Morris, D. W., Elkin, A., Muir, W.J., McGhee, K.A., Williamson, R., MacIntyre, D.J., MacLean, A.W., St, C.D., Robinson, M., Van Beck, M., Pereira, A.C., Kandaswamy, R., McQuillin, A., Collier, D.A., Bass, N.J., Young, A.H., Lawrence, J., Ferrier, I.N., Anjorin, A., Farmer, A., Curtis, D., Scolnick, E.M., McGuffin, P., Daly, M.J., Corvin, A.P., Holmans, P.A., Blackwood, D.H., Gurling, H.M., Owen, M.J., Purcell, S. M., Sklar, P., Craddock, N., Wellcome Trust Case Control, C, 2008. Collaborative genome-wide association analysis supports a role for ANK3 and CACNA1C in bipolar disorder. Nat. Genet. 40, 1056–1058.

Fountoulakis, K.N., Grunze, H., Vieta, E., Young, A., Yatham, L., Blier, P., Kasper, S., Moeller, H.J., 2017. The international college of neuro-psychopharmacology (CINP) treatment guidelines for bipolar disorder in adults (CINP-BD-2017), part 3: the clinical guidelines. Int. J. Neuropsychopharmacol. 20, 180–195.

Fountoulakis, K.N., Tohen, M., Zarate Jr., C.A., 2022. Lithium treatment of bipolar disorder in adults: a systematic review of randomized trials and meta-analyses. Eur. Neuropsychopharmacol. 54, 100–115.

Fuchs, C., Fustini, N., Trazzi, S., Gennaccaro, L., Rimondini, R., Ciani, E., 2018. Treatment with the GSK3-beta inhibitor tideglusib improves hippocampal development and memory performance in juvenile, but not adult, Cdkl5 knockout mice. Eur. J. Neurosci. 47, 1054–1066.

Garza, J.C., Qi, X., Gjeluci, K., Leussis, M.P., Basu, H., Reis, S.A., Zhao, W.N., Piguel, N. H., Penzes, P., Haggarty, S.J., Martens, G.J., Poelmans, G., Petryshen, T.L., 2018. Disruption of the psychiatric risk gene ankyrin 3 enhances microtubule dynamics through GSK3/CRMP2 signaling. Transl. Psychiatry 8, 135.

Gitlin, M., 2016. Lithium side effects and toxicity: prevalence and management strategies. Int J Bipolar Disord 4, 27.

Gonda, X., Pompili, M., Serafini, G., Montebovi, F., Campi, S., Dome, P., Duleba, T., Girardi, P., Rihmer, Z., 2012. Suicidal behavior in bipolar disorder: epidemiology, characteristics and major risk factors. J. Affect. Disord. 143, 16–26.

Gottschalk, M.G., Leussis, M.P., Ruland, T., Gjeluci, K., Petryshen, T.L., Bahn, S., 2017. Lithium reverses behavioral and axonal transport-related changes associated with ANK3 bipolar disorder gene disruption. Eur. Neuropsychopharmacol. 27, 274–288.

Huang, C.Y., Rasband, M.N., 2018. Axon initial segments: structure, function, and disease. Ann. N. Y. Acad. Sci. 1420, 46–61.

Jenkins, P.M., Bender, K.J., 2025. Axon initial segment structure and function in health and disease. Physiol. Rev. 105, 765–801.

Jope, R.S., Johnson, G.V., 2004. The glamour and gloom of glycogen synthase kinase-3. Trends Biochem. Sci. 29, 95–102.

Lee, M.T., Chen, C.H., Lee, C.S., Chen, C.C., Chong, M.Y., Ouyang, W.C., Chiu, N.Y., Chuo, L.J., Chen, C.Y., Tan, H.K., Lane, H.Y., Chang, T.J., Lin, C.H., Jou, S.H., Hou, Y.M., Feng, J., Lai, T.J., Tung, C.L., Chen, T.J., Chang, C.J., Lung, F.W., Chen, C.K., Shiah, I.S., Liu, C.Y., Teng, P.R., Chen, K.H., Shen, L.J., Cheng, C.S., Chang, T.P., Li, C.F., Chou, C.H., Chen, C.Y., Wang, K.H., Fann, C.S., Wu, J.Y., Chen, Y.T., Cheng, A.T., 2011. Genome-wide association study of bipolar I disorder in the han Chinese population. Mol. Psychiatr. 16, 548–556.

Merikangas, K.R., Jin, R., He, J.P., Kessler, R.C., Lee, S., Sampson, N.A., Viana, M.C., Andrade, L.H., Hu, C., Karam, E.G., Ladea, M., Medina-Mora, M.E., Ono, Y., Posada-Villa, J., Sagar, R., Wells, J.E., Zarkov, Z., 2011. Prevalence and correlates of bipolar spectrum disorder in the world mental health survey initiative. Arch. Gen. Psychiatry 68, 241–251.

Morales-Garcia, J.A., Luna-Medina, R., Alonso-Gil, S., Sanz-Sancristobal, M., Palomo, V., Gil, C., Santos, A., Martinez, A., Perez-Castillo, A., 2012. Glycogen synthase kinase 3 inhibition promotes adult hippocampal neurogenesis in vitro and in vivo. ACS Chem. Neurosci. 3, 963–971.

Muhleisen, T.W., Leber, M., Schulze, T.G., Strohmaier, J., Degenhardt, F., Treutlein, J., Mattheisen, M., Forstner, A.J., Schumacher, J., Breuer, R., Meier, S., Herms, S., Hoffmann, P., Lacour, A., Witt, S.H., Reif, A., Muller-Myhsok, B., Lucae, S., Maier, W., Schwarz, M., Vedder, H., Kammerer-Ciernioch, J., Pfennig, A., Bauer, M., Hautzinger, M., Moebus, S., Priebe, L., Czerski, P.M., Hauser, J., Lissowska, J., Szeszenia-Dabrowska, N., Brennan, P., McKay, J.D., Wright, A., Mitchell, P.B., Fullerton, J.M., Schofield, P.R., Montgomery, G.W., Medland, S.E., Gordon, S.D., Martin, N.G., Krasnow, V., Chuchalin, A., Babadjanova, G., Pantelejeva, G., Abramova, L.I., Tiganov, A.S., Polonikov, A., Khusnutdinova, E., Alda, M., Grof, P., Rouleau, G.A., Turecki, G., Laprise, C., Rivas, F., Mayoral, F., Kogevinas, M., Grigoroiu-Serbanescu, M., Propping, P., Becker, T., Rietschel, M., Nothen, M.M., Cichon, S., 2014. Genome-wide association study reveals two new risk loci for bipolar disorder. Nat. Commun. 5, 3339.

Mullins, N., Forstner, A.J., O'Connell, K.S., Coombes, B., Coleman, J.R.I., Qiao, Z., Als, T. D., Bigdeli, T.B., Borte, S., Bryois, J., Charney, A.W., Drange, O.K., Gandal, M.J., Hagenaars, S.P., Ikeda, M., Kamitaki, N., Kim, M., Krebs, K., Panagiotaropoulou, G., Schilder, B.M., Sloofman, L.G., Steinberg, S., Trubetskoy, V., Winsvold, B.S., Won, H. H., Abramova, L., Adorjan, K., Agerbo, E., Al Eissa, M., Albani, D., Alliey-Rodriguez, N., Anjorin, A., Antila, V., Antoniou, A., Awasthi, S., Baek, J.H., Baekvad-Hansen, M., Bass, N., Bauer, M., Beins, E.C., Bergen, S.E., Birner, A., Bocker Pedersen, C., Boen, E., Boks, M.P., Bosch, R., Brum, M., Brumpton, B.M., Brunkhorst-Kanaan, N., Budde, M., Bybjerg-Grauholm, J., Byerley, W., Cairns, M., Casas, M., Cervantes, P., Clarke, T.K., Cruceanu, C., Cuellar-Barboza, A., Cunningham, J., Curtis, D., Czerski, P.M., Dale, A.M., Dalkner, N., David, F.S., Degenhardt, F., Djurovic, S., Dobbyn, A.L., Douzenis, A., Elvsashagen, T., Escott-Price, V., Ferrier, I. N., Fiorentino, A., Foroud, T.M., Forty, L., Frank, J., Frei, O., Freimer, N.B., Frisen, L., Gade, K., Garnham, J., Gelernter, J., Giortz Pedersen, M., Gizer, I.R., Gordon, S.D., Gordon-Smith, K., Greenwood, T.A., Grove, J., Guzman-Parra, J., Ha, K., Haraldsson, M., Hautzinger, M., Heilbronner, U., Hellgren, D., Herms, S., Hoffmann, P., Holmans, P.A., Huckins, L., Jamain, S., Johnson, J.S., Kalman, J.L., Kamatani, Y., Kennedy, J., Kittel-Schneider, S., Knowles, J.A., Kogevinas, M., Koromina, M., Kranz, T.M., Kranzler, H.R., Kubo, M., Kupka, R., Kushner, S.A., Lavebratt, C., Lawrence, J., Leber, M., Lee, H.J., Lee, P.H., Levy, S.E., Lewis, C., Liao, C., Lucae, S., Lundberg, M., MacIntyre, D.J., Magnusson, S.H., Maier, W., Maihofer, A., Malaspina, D., Maratou, E., Martinsson, L., Mattheisen, M., McCarroll, S.A., McGregor, N.W., McGuffin, P., McKay, J.D., Medeiros, H., Medland, S.E., Millischer, V., Montgomery, G.W., Moran, J.L., Morris, D.W., Muhleisen, T.W., O'Brien, N., O'Donovan, C., Olde Loohuis, L.M., Oruc, L., Papiol, S., Pardinas, A.F., Perry, A., Pfennig, A., Porichi, E., Potash, J.B., Quested, D., Raj, T., Rapaport, M.H., DePaulo, J.R., Regeer, E.J., Rice, J.P., Rivas, F., Rivera, M., Roth, J., Roussos, P., Ruderfer, D.M., Sanchez-Mora, C., Schulte, E.C., Senner, F., Sharp, S., Shilling, P.D., Sigurdsson, E., Sirignano, L., Slaney, C., Smeland, O.B., Smith, D.J., Sobell, J.L., Soholm Hansen, C., Soler Artigas, M., Spijker, A.T., Stein, D. J., Strauss, J.S., Swiatkowska, B., Terao, C., Thorgeirsson, T.E., Toma, C., Tooney, P., Tsermpini, E.E., Vawter, M.P., Vedder, H., Walters, J.T.R., Witt, S.H., Xi, S., Xu, W., Yang, J.M.K., Young, A.H., Young, H., Zandi, P.P., Zhou, H., Zillich, L., Psychiatry, H. A.-I., Adolfsson, R., Agartz, I., Alda, M., Alfredsson, L., Babadjanova, G., Backlund, L., Baune, B.T., Bellivier, F., Bengesser, S., Berrettini, W.H., Blackwood, D. H.R., Boehnke, M., Borglum, A.D., Breen, G., Carr, V.J., Catts, S., Corvin, A., Craddock, N., Dannlowski, U., Dikeos, D., Esko, T., Etain, B., Ferentinos, P., Frye, M., Fullerton, J.M., Gawlik, M., Gershon, E.S., Goes, F.S., Green, M.J., Grigoroiu-Serbanescu, M., Hauser, J., Henskens, F., Hillert, J., Hong, K.S., Hougaard, D.M., Hultman, C.M., Hveem, K., Iwata, N., Jablensky, A.V., Jones, I., Jones, L.A., Kahn, R. S., Kelsoe, J.R., Kirov, G., Landen, M., Leboyer, M., Lewis, C.M., Li, Q.S., Lissowska, J., Lochner, C., Loughland, C., Martin, N.G., Mathews, C.A., Mayoral, F., McElroy, S.L., McIntosh, A.M., McMahon, F.J., Melle, I., Michie, P., Milani, L., Mitchell, P.B., Morken, G., Mors, O., Mortensen, P.B., Mowry, B., Muller-Myhsok, B., Myers, R.M., Neale, B.M., Nievergelt, C.M., Nordentoft, M., Nothen, M.M., O'Donovan, M.C., Oedegaard, K.J., Olsson, T., Owen, M.J., Paciga, S.A., Pantelis, C., Pato, C., Pato, M.T., Patrinos, G.P., Perlis, R.H., Posthuma, D., Ramos-Quiroga, J.A., Reif, A., Reininghaus, E.Z., Ribases, M., Rietschel, M., Ripke, S., Rouleau, G.A., Saito, T., Schall, U., Schalling, M., Schofield, P.R., Schulze, T.G., Scott, L.J., Scott, R. J., Serretti, A., Shannon Weickert, C., Smoller, J.W., Stefansson, H., Stefansson, K., Stordal, E., Streit, F., Sullivan, P.F., Turecki, G., Vaaler, A.E., Vieta, E., Vincent, J.B., Waldman, I.D., Weickert, T.W., Werge, T., Wray, N.R., Zwart, J.A., Biernacka, J.M., Nurnberger, J.I., Cichon, S., Edenberg, H.J., Stahl, E.A., McQuillin, A., Di Florio, A., Ophoff, R.A., Andreassen, O.A., 2021. Genome-wide association study of more than 40,000 bipolar disorder cases provides new insights into the underlying biology. Nat. Genet. 53, 817–829.

Nelson, A.D., Caballero-Floran, R.N., Rodriguez Diaz, J.C., Hull, J.M., Yuan, Y., Li, J., Chen, K., Walder, K.K., Lopez-Santiago, L.F., Bennett, V., McInnis, M.G., Isom, L.L., Wang, C., Zhang, M., Jones, K.S., Jenkins, P.M., 2020. Ankyrin-G regulates forebrain connectivity and network synchronization via interaction with GABARAP. Mol. Psychiatr. 25, 2800–2817.

Nelson, A.D., Jenkins, P.M., 2017. Axonal membranes and their domains: assembly and function of the axon initial segment and node of ranvier. Front. Cell. Neurosci. 11, 136.

Nestsiarovich, A., Gaudiot, C.E.S., Baldessarini, R.J., Vieta, E., Zhu, Y., Tohen, M., 2022. Preventing new episodes of bipolar disorder in adults: systematic review and meta-analysis of randomized controlled trials. Eur. Neuropsychopharmacol. 54, 75–89.

Nolen, W.A., Licht, R.W., Young, A.H., Malhi, G.S., Tohen, M., Vieta, E., Kupka, R.W., Zarate, C., Nielsen, R.E., Baldessarini, R.J., Severus, E., ISBD/IGSLI Task Force on the treatment with lithium, 2019. What is the optimal serum level for lithium in the maintenance treatment of bipolar disorder? A systematic review and recommendations from the ISBD/IGSLI task force on treatment with lithium. Bipolar Disord. 21, 394–409.

Oldis, M., Murray, G., Macneil, C.A., Hasty, M.K., Daglas, R., Berk, M., Conus, P., Cotton, S.M., 2016. Trajectory and predictors of quality of life in first episode psychotic mania. J. Affect. Disord. 195, 148–155.

Organization, W.H., 1993. The ICD-10 Classification of Mental and Behavioural Disorders: Diagnostic Criteria for Research. World Health Organization, Geneva, Switzerland.

Ozerdema, A., Guntekind, B., Atagune, M.I., Basar, E., 2013. Brain oscillations in bipolar disorder in search of new biomarkers. Suppl. Clin. neurophysiol. 62, 207–221.

Paxinos, G., Franklin, K.B.J., 2019. Paxinos and Franklin's the Mouse Brain in Stereotaxic Coordinates. Elsevier Science & Technology, San Diego.

Piguel, N.H., Yoon, S., Gao, R., Horan, K.E., Garza, J.C., Petryshen, T.L., Smith, K.R., Penzes, P., 2023. Lithium rescues dendritic abnormalities in Ank3 deficiency models through the synergic effects of GSK3beta and cyclic AMP signaling pathways. Neuropsychopharmacology 48, 1000–1010.

Psychiatric GWAS Consortium Bipolar Disorder Working Group, 2011. Large-scale genome-wide association analysis of bipolar disorder identifies a new susceptibility locus near ODZ4. Nat. Genet. 43, 977–983.

Roshanaei-Moghaddam, B., Katon, W., 2009. Premature mortality from general medical illnesses among persons with bipolar disorder: a review. Psychiatr. Serv. 60, 147–156.

Schaffer, A., Isometsa, E.T., Tondo, L., D, H.M., Turecki, G., Reis, C., Cassidy, F., Sinyor, M., Azorin, J.M., Kessing, L.V., Ha, K., Goldstein, T., Weizman, A., Beautrais, A., Chou, Y.H., Diazgranados, N., Levitt, A.J., Zarate Jr., C.A., Rihmer, Z., Yatham, L.N., 2015. International society for bipolar disorders task force on suicide: meta-analyses and meta-regression of correlates of suicide attempts and suicide deaths in bipolar disorder. Bipolar Disord. 17, 1–16.

Schubert, K.O., Focking, M., Cotter, D.R., 2015. Proteomic pathway analysis of the hippocampus in schizophrenia and bipolar affective disorder implicates 14-3-3 signaling, aryl hydrocarbon receptor signaling, and glucose metabolism: potential roles in GABAergic interneuron pathology. Schizophr. Res. 167, 64–72.

Sereno, L., Coma, M., Rodriguez, M., Sanchez-Ferrer, P., Sanchez, M.B., Gich, I., Agullo, J.M., Perez, M., Avila, J., Guardia-Laguarta, C., Clarimon, J., Lleo, A., Gomez-Isla, T., 2009. A novel GSK-3beta inhibitor reduces Alzheimer's pathology and rescues neuronal loss in vivo. Neurobiol. Dis. 35, 359–367.

Shorter, E., 2009. The history of lithium therapy. Bipolar Disord. 11 (Suppl. 2), 4–9.

Smith, K.R., Penzes, P., 2018. Ankyrins: roles in synaptic biology and pathology. Mol. Cell. Neurosci. 91, 131–139.

Smoller, J.W., Finn, C.T., 2003. Family, twin, and adoption studies of bipolar disorder. Am J Med Genet C Semin Med Genet 123C, 48–58.

Stahl, E.A., Breen, G., Forstner, A.J., McQuillin, A., Ripke, S., Trubetskoy, V., Mattheisen, M., Wang, Y., Coleman, J.R.I., Gaspar, H.A., de Leeuw, C.A., Steinberg, S., Pavlides, J.M.W., Trzaskowski, M., Byrne, E.M., Pers, T.H., Holmans, P. A., Richards, A.L., Abbott, L., Agerbo, E., Akil, H., Albani, D., Alliey-Rodriguez, N., Als, T.D., Anjorin, A., Antila, V., Awasthi, S., Badner, J.A., Baekvad-Hansen, M., Barchas, J.D., Bass, N., Bauer, M., Belliveau, R., Bergen, S.E., Pedersen, C.B., Boen, E., Boks, M.P., Boocock, J., Budde, M., Bunney, W., Burmeister, M., Bybjerg-Grauholm, J., Byerley, W., Casas, M., Cerrato, F., Cervantes, P., Chambert, K., Charney, A.W., Chen, D., Churchhouse, C., Clarke, T.K., Coryell, W., Craig, D.W., Cruceanu, C., Curtis, D., Czerski, P.M., Dale, A.M., de Jong, S., Degenhardt, F., Del-Favero, J., DePaulo, J.R., Djurovic, S., Dobbyn, A.L., Dumont, A., Elvsashagen, T., Escott-Price, V., Fan, C.C., Fischer, S.B., Flickinger, M., Foroud, T.M., Forty, L., Frank, J., Fraser, C., Freimer, N.B., Frisen, L., Gade, K., Gage, D., Garnham, J., Giambartolomei, C., Pedersen, M.G., Goldstein, J., Gordon, S.D., Gordon-Smith, K., Green, E.K., Green, M.J., Greenwood, T.A., Grove, J., Guan, W., Guzman-Parra, J., Hamshere, M.L., Hautzinger, M., Heilbronner, U., Herms, S., Hipolito, M., Hoffmann, P., Holland, D., Huckins, L., Jamain, S., Johnson, J.S., Jureus, A., Kandaswamy, R., Karlsson, R., Kennedy, J.L., Kittel-Schneider, S., Knowles, J.A., Kogevinas, M., Koller, A.C., Kupka, R., Lavebratt, C., Lawrence, J., Lawson, W.B., Leber, M., Lee, P.H., Levy, S.E., Li, J.Z., Liu, C., Lucae, S., Maaser, A., MacIntyre, D. J., Mahon, P.B., Maier, W., Martinsson, L., McCarroll, S., McGuffin, P., McInnis, M. G., McKay, J.D., Medeiros, H., Medland, S.E., Meng, F., Milani, L., Montgomery, G. W., Morris, D.W., Muhleisen, T.W., Mullins, N., Nguyen, H., Nievergelt, C.M., Adolfsson, A.N., Nwulia, E.A., O'Donovan, C., Loohuis, L.M.O., Ori, A.P.S., Oruc, L., Osby, U., Perlis, R.H., Perry, A., Pfennig, A., Potash, J.B., Purcell, S.M., Regeer, E.J., Reif, A., Reinbold, C.S., Rice, J.P., Rivas, F., Rivera, M., Roussos, P., Ruderfer, D.M., Ryu, E., Sanchez-Mora, C., Schatzberg, A.F., Scheftner, W.A., Schork, N.J., Shannon Weickert, C., Shehktman, T., Shilling, P.D., Sigurdsson, E., Slaney, C., Smeland, O.B., Sobell, J.L., Soholm Hansen, C., Spijker, A.T., St Clair, D., Steffens, M., Strauss, J.S., Streit, F., Strohmaier, J., Szelinger, S., Thompson, R.C., Thorgeirsson, T.E., Treutlein, J., Vedder, H., Wang, W., Watson, S.J., Weickert, T.W., Witt, S.H., Xi, S., Xu, W., Young, A.H., Zandi, P., Zhang, P., Zollner, S., e, Q.C., Consortium, B., Adolfsson, R., Agartz, I., Alda, M., Backlund, L., Baune, B.T., Bellivier, F., Berrettini, W.H., Biernacka, J.M., Blackwood, D.H.R., Boehnke, M., Borglum, A.D., Corvin, A., Craddock, N., Daly, M.J., Dannlowski, U., Esko, T., Etain, B., Frye, M., Fullerton, J.M., Gershon, E.S., Gill, M., Goes, F., Grigoroiu-Serbanescu, M., Hauser, J., Hougaard, D.M., Hultman, C.M., Jones, I., Jones, L.A., Kahn, R.S., Kirov, G., Landen, M., Leboyer, M., Lewis, C.M., Li, Q.S., Lissowska, J., Martin, N.G., Mayoral, F., McElroy, S.L., McIntosh, A.M., McMahon, F.J., Melle, I., Metspalu, A., Mitchell, P.B., Morken, G., Mors, O., Mortensen, P.B., Muller-Myhsok, B., Myers, R. M., Neale, B.M., Nimgaonkar, V., Nordentoft, M., Nothen, M.M., O'Donovan, M.C., Oedegaard, K.J., Owen, M.J., Paciga, S.A., Pato, C., Pato, M.T., Posthuma, D., Ramos-Quiroga, J.A., Ribases, M., Rietschel, M., Rouleau, G.A., Schalling, M., Schofield, P.R., Schulze, T.G., Serretti, A., Smoller, J.W., Stefansson, H., Stefansson, K., Stordal, E., Sullivan, P.F., Turecki, G., Vaaler, A.E., Vieta, E., Vincent, J.B., Werge, T., Nurnberger, J.I., Wray, N.R., Di Florio, A., Edenberg, H.J., Cichon, S., Ophoff, R.A., Scott, L.J., Andreassen, O.A., Kelsoe, J., Sklar, P., Bipolar

Disorder Working Group of the Psychiatric Genomics, C., 2019. Genome-wide association study identifies 30 loci associated with bipolar disorder. Nat. Genet. 51, 793–803.

Stevens, S.R., Rasband, M.N., 2021. Ankyrins and neurological disease. Curr. Opin. Neurobiol. 69, 51–57.

Stevens, S.R., Rasband, M.N., 2022. Pleiotropic ankyrins: scaffolds for ion channels and transporters. Channels 16, 216–229.

Tamas, G., Buhl, E.H., Lorincz, A., Somogyi, P., 2000. Proximally targeted GABAergic synapses and gap junctions synchronize cortical interneurons. Nat. Neurosci. 3, 366–371.

Torrey, E.F., Barci, B.M., Webster, M.J., Bartko, J.J., Meador-Woodruff, J.H., Knable, M. B., 2005. Neurochemical markers for schizophrenia, bipolar disorder, and major depression in postmortem brains. Biol. Psychiatry 57, 252–260.

Tseng, W.C., Jenkins, P.M., Tanaka, M., Mooney, R., Bennett, V., 2015. Giant ankyrin-G stabilizes somatodendritic GABAergic synapses through opposing endocytosis of GABAA receptors. Proc. Natl. Acad. Sci. U. S. A. 112, 1214–1219.

Tyagarajan, S.K., Ghosh, H., Yevenes, G.E., Nikonenko, I., Ebeling, C., Schwerdel, C., Sidler, C., Zeilhofer, H.U., Gerrits, B., Muller, D., Fritschy, J.M., 2011. Regulation of GABAergic synapse formation and plasticity by GSK3beta-dependent phosphorylation of gephyrin. Proc. Natl. Acad. Sci. U. S. A. 108, 379–384.

Villacres, J.E., Riveira, N., Kim, S., Colgin, L.L., Noebels, J.L., Lopez, A.Y., 2023. Abnormal patterns of sleep and waking behaviors are accompanied by neocortical oscillation disturbances in an Ank3 mouse model of epilepsy-bipolar disorder comorbidity. Transl. Psychiatry 13, 403.

Yatham, L.N., Kennedy, S.H., Parikh, S.V., Schaffer, A., Bond, D.J., Frey, B.N., Sharma, V., Goldstein, B.I., Rej, S., Beaulieu, S., Alda, M., MacQueen, G., Milev, R.V., Ravindran, A., O'Donovan, C., McIntosh, D., Lam, R.W., Vazquez, G., Kapczinski, F., McIntyre, R.S., Kozicky, J., Kanba, S., Lafer, B., Suppes, T., Calabrese, J.R., Vieta, E., Malhi, G., Post, R.M., Berk, M., 2018. Canadian network for mood and anxiety treatments (CANMAT) and international society for bipolar disorders (ISBD) 2018 guidelines for the management of patients with bipolar disorder. Bipolar Disord. 20, 97–170.

Zhu, S., Cordner, Z.A., Xiong, J., Chiu, C.T., Artola, A., Zuo, Y., Nelson, A.D., Kim, T.Y., Zaika, N., Woolums, B.M., Hess, E.J., Wang, X., Chuang, D.M., Pletnikov, M.M., Jenkins, P.M., Tamashiro, K.L., Ross, C.A., 2017. Genetic disruption of ankyrin-G in adult mouse forebrain causes cortical synapse alteration and behavior reminiscent of bipolar disorder. Proc. Natl. Acad. Sci. U. S. A. 114, 10479–10484.
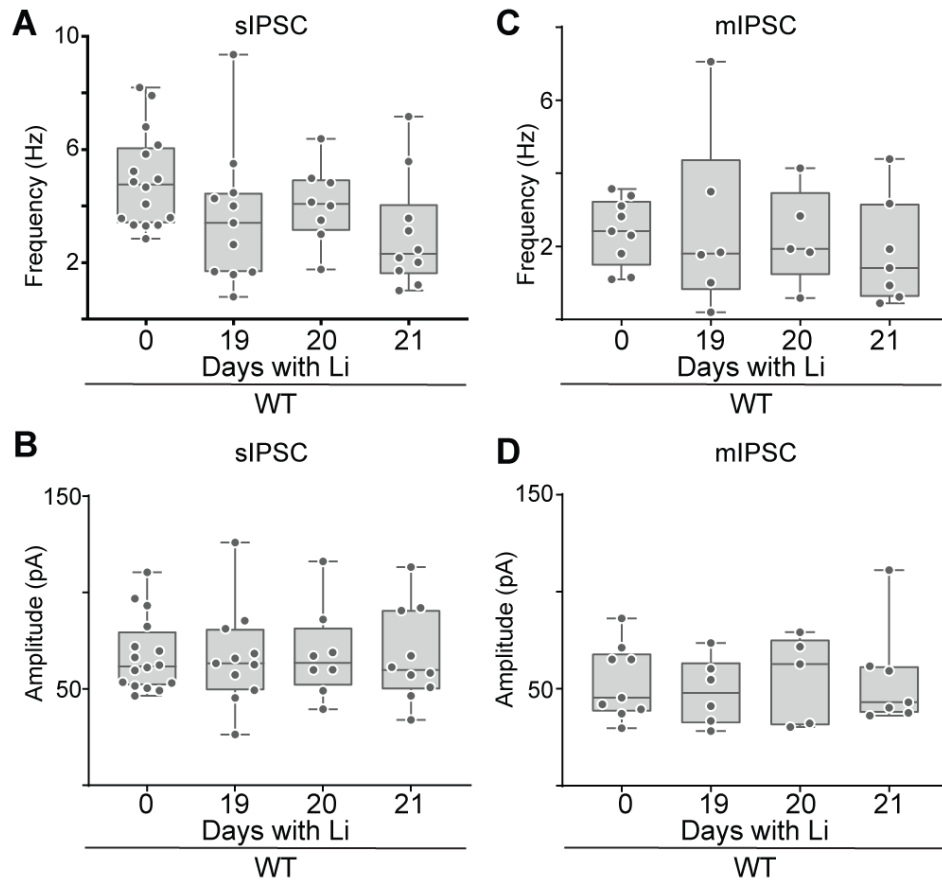
**Figure S1. Chronic lithium treatment does not affect IPSC frequency or amplitude in WT mice.** (A) Quantification of sIPSC frequency (Hz) from cortical neurons from brain slices of WT mice without treatment and after chronic lithium treatment 19-21 days: Ordinary one-way ANOVA ($F_{(3, 41)}$ = 2.326, P = 0.0889). (WT: n=16; WT/Day 19 + Li: n=12; WT/Day 20 + Li: n=8 and WT/Day 21 + Li n=10) (B) and amplitude (pA): Ordinary one-way ANOVA ($F_{(3, 41)}$ = 0.1093, P = 0.9542). (WT: n=16; WT/Day 19 + Li: n=11; WT/Day 20 + Li: n=8 and WT/Day 21 + Li n=10). (C) Quantification of mIPSC frequency (Hz) of WT (gray) and WT after chronic lithium treatment 19-21 days. Ordinary one-way ANOVA ($F_{(3, 23)}$ = 0.2659, P=0.8492) (D) and amplitude (pA): Ordinary one-way ANOVA ($F_{(3, 41)}$ = 0.5547, P=0.6479), (WT: n=9; WT/Day 19 + Li: n=6; WT/Day 20 + Li: n=5 and WT/Day 21 + Li n=7). N=3-6 mice.
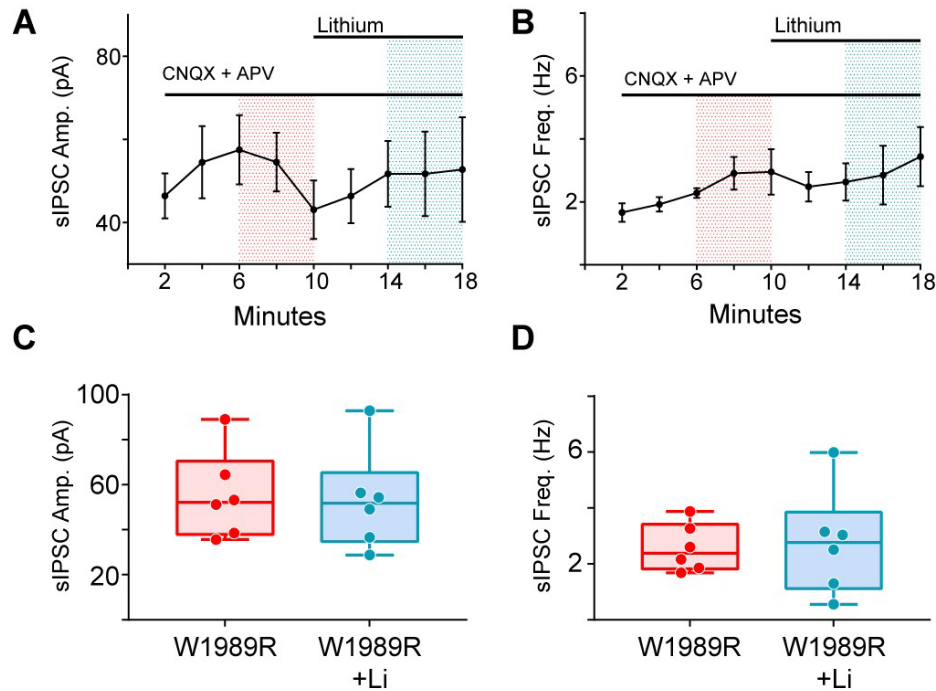
**Figure S2. Acute lithium treatment does not modify sIPSCs in layer II/III cortical neurons from *Ank3* p.W1989R mice.** (A) The temporal curve of sIPSC amplitude (pA) and (B) frequency (Hz) in response to acute lithium (0.8mmol/L) for 8 minutes. (C) Quantification of the sIPSC amplitude (pA) (T-test (t=0.1916, df=10, P= 0.852) in (A). Quantification of the sIPSC frequency (Hz) (T-test (t=0.2119, df=10, P= 0.836)) in (B). *Ank3* p.W1989R (W1989R) (red), and *Ank3* p.W1989R in the presence of lithium (W1989R +Li) (blue) in acute brain slices. (W1989R: n=6; W1989R + Li: n=6). For quantification in plots (A) and (C) the average from minutes 4-8 was estimated as a control and 14-18 minutes for the lithium condition. N=2 mice.
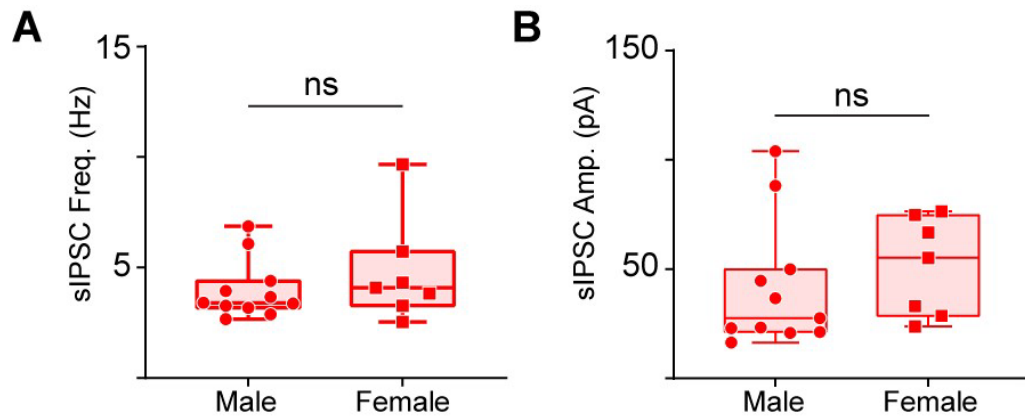
**Figure S3. Lithium treatment causes identical effects in male and female *Ank3* p.W1989R mice.** (A) sIPSC frequency (Hz) and (B) amplitude (pA) in response to acute lithium treatment for 21 days, in acute brain slices from Males (red circles) and females (red squares). Mann Whitney test P = ns (Males n=11 and Females n = 7).

**A** Electrophysiological properties of the first AP from AP train in Figure 4

| | Membrane Potential (mV) | Rheobase (pA) | Threshold (mV) | Amplitude (mV) | Width (ms) | dV/dt Depolarization | dV/dt Repolarization |
|---|---|---|---|---|---|---|---|
| Wild type | -64.34 ± 2.74 (n=7) | 55.71 ± 17.16 (n=7) | -46.26 ± 3.23 (n=7) | 104.6 ± 12.43 (n=7) | 2.56 ± 0.31 (n=7) | 176.0 ± 66.71 (n=7) | -37.07 ± 7.48 (n=7) |
| W1989R | -66.93 ± 6.30 (n=12) | 41.67 ± 7.76 (n=12) | -43.33 ± 2.61 (n=12) | 112.8 ± 13.31 (n=12) | 2.52 ± 0.60 (n=12) | 189.9 ± 44.72 (n=12) | -41.30 ± 8.84 (n=12) |
| W1989R+Li | -67.90 ± 4.10 (n=15) | 48.67 ± 8.55 (n=15) | -41.41 ± 3.19** (n=15) | 109.2 ± 9.27 (n=15) | 2.90 ± 0.57 (n=15) | 158.2 ± 54.55 (n=15) | -34.39 ± 8.2 (n=15) |

**B**



— WT
— W1989R
— W1989R + Li

20mV
5ms
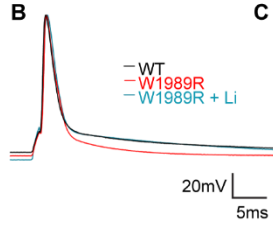
**C** Electrophysiological properties from single evoked AP

| | Membrane Potential (mV) | Membrane Resistance (mΩ) | Threshold (mV) | Amplitude (mV) | Width (ms) | dV/dt Depolarization | dV/dt Repolarization |
|---|---|---|---|---|---|---|---|
| Wild type | -66.08 ± 5.58 (n=13) | 123.4 ± 55.83 (n=12) | -48.23 ± 5.66 (n=13) | 110.1 ± 11.15 (n=13) | 2.25 ± 0.53 (n=13) | 233.90 ± 72.78 (n=13) | -44.53 ± 14.08 (n=13) |
| W1989R | -67.65 ± 5.62 (n=25) | 152.8 ± 51.47 (n=22) | -46.13 ± 4.33 (n=25) | 111.17 ± 12.91 (n=25) | 2.47 ± 0.37 (n=25) | 197.3 ± 47.13 (n=25) | -37.84 ± 6.83 (n=25) |
| W1989R+Li | -69.67 ± 4.71 (n=13) | 166.9 ± 52.24 (n=13) | -44.21 ± 6.25 (n=13) | 114.1 ± 6.69 (n=13) | 2.37 ± 0.46 (n=13) | 199.3 ± 51.04 (n=13) | -43.24 ± 10.75 (n=13) |

**Figure S4.**

**Effect of lithium treatment on single action potential (AP) properties.**

(A) Quantification of electrophysiological properties from the first AP in train shown in Figure 4 from layer II/III cortical pyramidal neurons in acute brain slices from wild-type (WT) and *Ank3* pW1989R homozygous mice with (W1989R+Li) or without lithium treatment (W1989R). Membrane potential: Ordinary one-way ANOVA (F (2, 31) = 1.308, P=0.2850). Rheobase: Ordinary one-way ANOVA (F (2, 31) = 0.3908, P=0.6798). Threshold: Ordinary one-way ANOVA (F (2, 31) = 6.251, P=0.0052). Tukey's multiple comparisons tests (**P= 0.0038 in WT vs. W1989R + Lithium). Amplitude: Ordinary one-way ANOVA (F (2, 31) = 1.152, P=0.3291). Width: Ordinary one-way ANOVA (F (2, 31) = 1.853, P=0.1738). dV/dt Depolarization: Ordinary one-way ANOVA (F (2, 31) = 1.157, P=0.3276). dV/dt Repolarization: Ordinary one-way ANOVA (F (2, 31) = 2.316, P=0.1155). (B) Representative single evoked APs from layer II/III cortical pyramidal neurons in acute brain slices from wild-type (WT) and *Ank3* pW1989R homozygous mice with (W1989R+Li) or without lithium treatment (W1989R). (C) Electrophysiological properties from evoked single APs. Membrane potential: Ordinary one-way ANOVA (F (2, 48) = 1.438, P=0.2474). Membrane resistance: Ordinary one-way ANOVA (F (2, 44) = 2.213, P=0.1214). Threshold: Ordinary one-way ANOVA (F (2, 48) = 1.933, P=0.1558). Amplitude: Ordinary one-way ANOVA (F (2, 48) = 0.4152, P=0.6626). Width: Ordinary one-way ANOVA (F (2, 48) = 1.098, P=0.3417). dV/dt Depolarization: Ordinary one-way ANOVA (F (2, 48) = 2.030, P=0.1424). dV/dt Repolarization: Ordinary one-way ANOVA (F (2, 48) = 2.340, P=0.1072). The 'n' represents the number of individual neurons per parameter in each condition. N=3-6 mice.